Materials Research Proceedings 28 (2023) 919-928 https://doi.org/10.21741/9781644902479-100

Numerical investigation on the deep drawing of sheet metals with an additively applied coating

MÄRZ Raphaela[1,a *], HAFENECKER Jan[1,b], BARTELS Dominic[2,3,c], SCHMIDT Michael[2,3,d] and MERKLEIN Marion[1,e]

[1]Institute of Manufacturing Technology (LFT), Friedrich-Alexander-Universität Erlangen-Nürnberg, Egerlandstraße 13, 91058 Erlangen, Germany

[2]Institute of Photonic Technologies (LPT), Friedrich-Alexander-Universität Erlangen-Nürnberg, Konrad-Zuse-Straße 3/5, 91052 Erlangen, Germany

[3] Erlangen Graduate School in Advanced Optical Technologies (SAOT), Paul-Gordan-Straße 6, 91052 Erlangen, Germany

[a]raphaela.maerz@fau.de, [b]jan.hafenecker@fau.de, [c]dominic.bartels@lpt.uni-erlangen.de, [d]m.schmidt@blz.org, [e]marion.merklein@fau.de

Keywords: Additive Manufacturing, Forming, Hybrid Parts

Abstract. A promising approach to meet ecological and economical challenges in production industry is the combination of additive manufacturing and forming, which enables the production of hybrid parts. The fusion of the two technologies has the potential to use the benefits of both process classes. One example for the combination of additive manufacturing and forming is a process chain consisting of laser-based directed energy deposition (DED-LB/M) to apply a wear resistant coating on a sheet metal and a subsequent deep drawing process to achieve the final geometry of the component. However, the presence of the local reinforcement influences the subsequent sheet metal forming process. In order to gain more knowledge about the process chain a numerical approach is performed. In this work, the influence of a coating using Bainidur® AM applied by DED-LB/M on the formability of the case hardening steel 16MnCr5 in a deep drawing process is evaluated. For this purpose, a numerical model is built and validated by comparison with experimental results. The finite-element-model serves as the basis for the investigation on the influence of the location of the additively applied coating on the deep drawing process and also enables a deeper understanding of the process.

Introduction

Due to governmental requirements and an increasing environmental awareness, modern production technology has to face new ecological and economical challenges [1]. Therefore, a need for resource efficiency and sustainability in the field of production is coming into focus. In addition to lightweight design [2] another approach to meet the current challenges are resource efficient manufacturing processes. Forming technology is known for its resource efficiency as well as for the high output [3]. On the other hand, a disadvantage of the production technology is its low flexibility [3]. In contrast, the use of additive manufacturing enables a high degree of geometric freedom and a customizability of the components [4]. By combining the two technologies, a production of hybrid parts is possible. Synergy effects such as adapted material properties as well as an extension of the process limits appear and the disadvantages of the two process classes can be compensated [5]. One example for the production of hybrid parts is a process chain consisting of DED-LB/M to apply a wear-resistant coating on a circular blank and a subsequent deep drawing process to achieve the final geometry of the component, which is based on the geometry of a barrel sleeve. The forming process enables a resource efficient production of the component compared to current machining of the barrel sleeve. The use of DED-LB/M before

the forming process enables a local reinforcement of the blank. Therefore, global energy-intensive heat treatment strategies can be avoided. The authors in [6] show that DED-LB/M can be used to locally strengthen aluminum sheet metal blanks. The formability of the aluminum blanks is limited due to the heat input [6]. Nevertheless, no investigations have yet been carried out into how a high-strength material applied by DED-LB/M affects the formability of a case hardening steel.

Objective and Methodology

The aim of this work is to investigate the influence of an additively applied coating on a deep drawing process. This is necessary to evaluate the formability of hybrid components where a high-strength coating is applied. The methodology used in this work is shown in Fig.1.

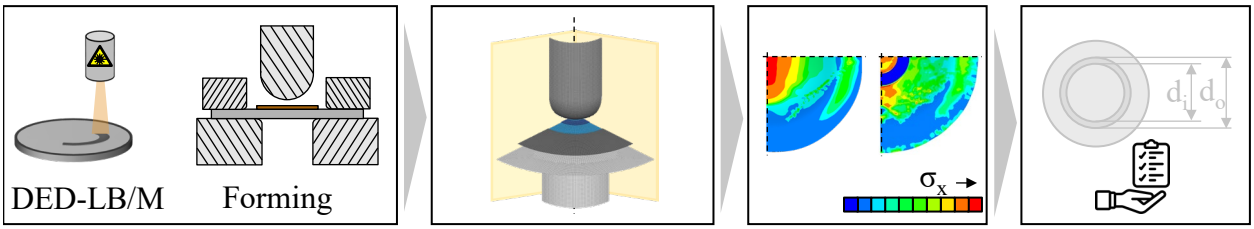

Fig.1. Methodology.

The basis of the investigation is a process combination of DED-LB/M and a subsequent deep drawing process. In a first step, a FE-model of the forming process is built. In addition to the conventional deep drawing process, the model is extended to include the hybrid approach. The validation is done by comparison with experimental results. In addition to the process force, the geometry of the component is compared in order to evaluate the prediction quality of the FE-model. After the validation, an investigation of the stress state of the uncoated and hybrid components is carried out in order to derive conclusions about the formability of hybrid components and the advantageous placement of the additive coating.

Experimental and Numerical Setup

Material and semi-finished product. To produce the hybrid part a process chain consisting of DED-LB/M and a subsequent deep drawing process is used. The geometry of the semi-finished part is shown in Fig. 2a. A circular blank with a diameter of 105 mm and a thickness of 3.5 mm serves as substrate. As material the case hardening steel 16MnCr5 (1.7131) is used. Before the deep drawing process, a wear-resistant coating is applied on the sheet by DED-LB/M. Therefore, the metal powder Bainidur® AM is used. The applied geometry is shown with its variations in Fig. 2b.

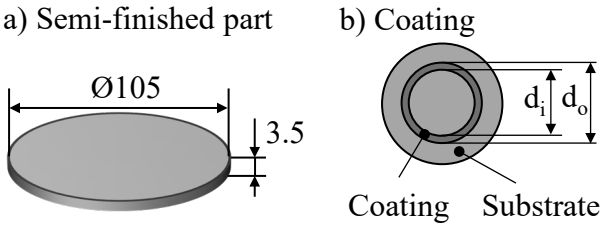

Coating	Inner diameter d_i	Outer diameter d_o
small	16 mm	27 mm
medium	24 mm	35 mm
large	32 mm	43 mm

Fig. 2. a) Geometry of the semi-finished part b) Geometry of the coating and its variations.

The coating is applied in a circle and has a height of 0.5 mm. A difference is made between the listed inner and outer diameters in order to determine the influence of the position of the coating on the forming process. To describe the mechanical properties and the hardening behavior of the substrate material and the coating, true stress-true plastic strain curves are determined, which are used for the numerical simulation. The resulting curves are shown in Fig. 3.

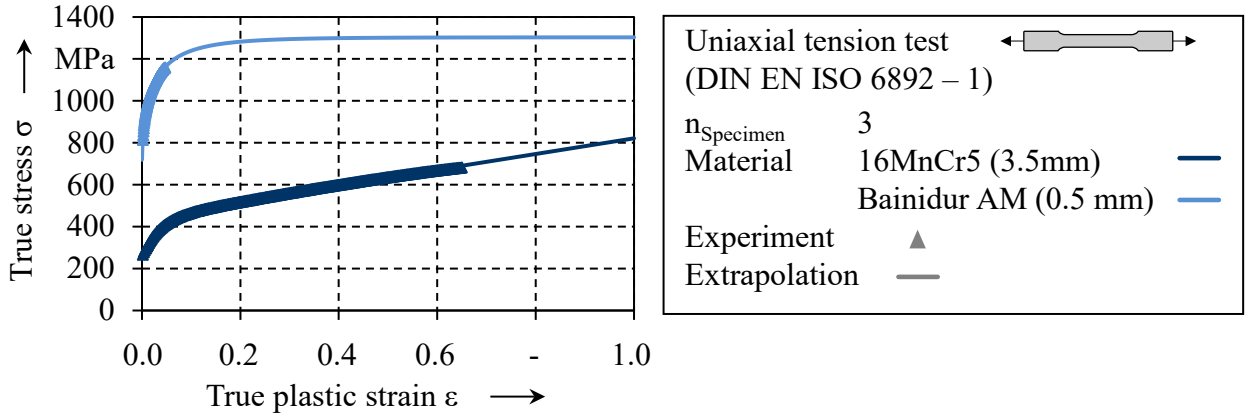

Fig. 3. True stress-true plastic strain curves of the substrate material 16MnCr5 and the coating Bainidur® AM from experimental uniaxial tension tests.

Due to the prevailing stress conditions in deep drawing processes, uniaxial tension tests according to DIN EN ISO 6892-1 [7] at room temperature are carried out. The specimens for the characterization of the substrate material have a measuring length of 50 mm and a width of 12.5 mm. Tensile specimens are also used to characterize the coating. Due to the dimensions of the coating, a smaller specimen geometry with a measuring length of 20 mm and a width of 6 mm is used. The thickness of the specimens corresponds to the thickness of the coating in the experiment. The specimens were first built up as a block through five layers and in the second step separated from the substrate and brought to the final shape by electrical discharge machining. The uniaxial tension tests are carried out using a universal testing machine Zwick Z100 respectively Zwick Z10 for the smaller specimens and a camera-based 3D strain measuring system GOM Aramis. The substrate has a significantly lower initial yield stress of 266 MPa than the coating with a yield stress of 814 MPa. Since higher strains than those determined experimentally

occur in the real process, the two curves were approximated and extrapolated. Voce generalized [8] is chosen as extrapolation approach for the substrate material 16MnCr5. For the coating, the Hockett-Sherby approach [9] was found to be appropriate.

Laser-based directed energy deposition. Before the forming process, circular blanks are coated using DED-LB/M. Therefore, the experiments are performed on an ERLAS UNIVERSAL 50349 machine (ERLAS GmbH). The machine is equipped with a diode laser with a peak power of 4 kW and a characteristic wavelength of 900 to 1080 nm. The nozzle can be moved using three linear axes. In addition, the cell has a sample holder with two rotary axes, which allows the realization of free-form surfaces. The parameter set used for the coating is based on previous investigations [10].

Deep drawing. The subsequent deep drawing process is carried out on a hydraulic press Lasco TSP 100 So with a maximum force up to 1000 kN. The velocity of the punch is set to 4.7 mm/s and the force of the binder is set to 25 kN. The punch geometry is hemispherical with a diameter of 50 mm. The drawing depth, which is set by hard-stops, amounts to 30 mm. In order to reduce the tribological loads, the blanks are lubricated with KTL N 16. The experiments are carried out at room temperature. After the forming process, the parts are measured optically in order to determine the geometry and the sheet thickness. The measurement is carried out with an Atos Core 300 of the company GOM GmbH.

Numerical setup. The numerical model presented in this paper is built with the finite element software LS-Dyna by Ansys, which allows the simulation of nonlinear physical processes. The generation of the input is done with the help of the graphical pre- and post-processor LS-PrePost V.4.7.0. As solver the MPP Double R11.1 is used. Due to the symmetry of the hybrid part, only a quarter is modelled. Therefore, the Keyword “SPC_SET” is applied to the nodes on the x- and y-edges of the part and the coating. For the tools, namely punch, binder and die, rigid shell elements are used. To avoid unwanted movement, constraints in x- and y-direction are defined for the tools. The numerical setup is shown in Fig. 4.

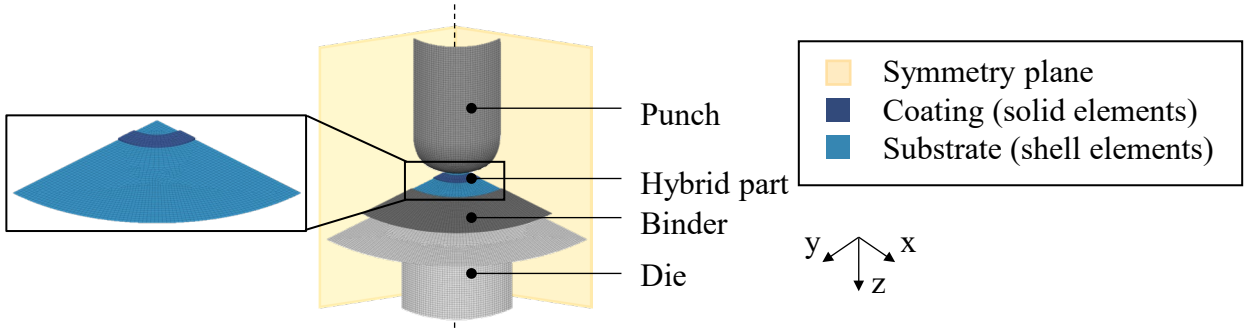

Fig. 4. Setup of numerical model to map the deep drawing process.

The sheet is modeled by fully integrated shell elements. As material model “133-Barlat_YLD2000” is used due to the anisotropic material behavior of the case hardening steel 16MnCr5. In order to map the coating, the material keyword “024-PIECEWISE_LINEAR_PLASTICITY” is applied. In contrast to the substrate material, the coating is modeled with solid elements. To consider the adhesion of the coating to the substrate, the two parts share the same transition nodes. This approach is also chosen in [11]. The contact is modeled with the keyword “CONTACT_FORMING_SURFACE_TO_SURFACE” to avoid penetrations between the tools and the blank.

Results

Validation. In order to evaluate the prediction quality of the presented FE-model, it is validated by comparison with experimental results. In addition to the hybrid part, the conventional deep drawing process is also considered. In Fig. 5, the comparison of the experimentally and numerically determined maximum process forces is shown.

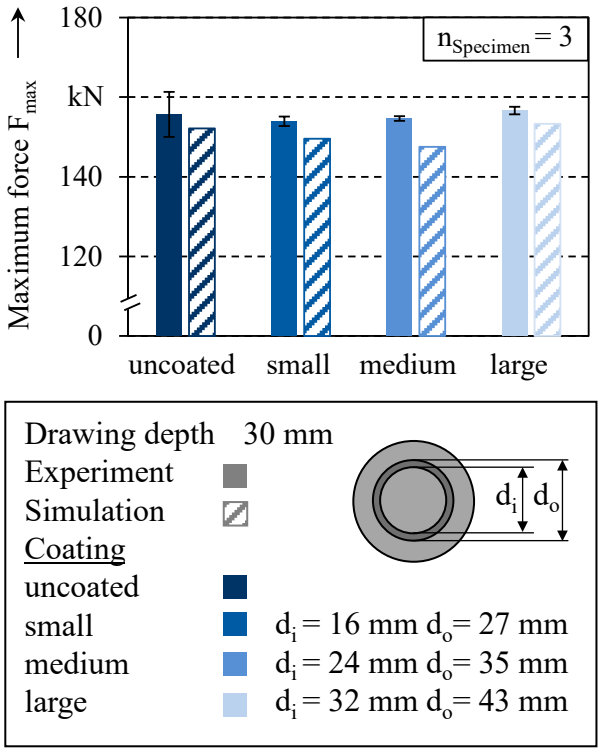

Fig. 5. Comparison of experimental and numerical maximum process force.

Experimentally, a maximum forming force of 155.7 ± 5.1 kN is determined while forming the uncoated blank. In the simulation a maximum forming force of 152.1 kN is reached. With a deviation of 2.6 %, a good agreement between the simulation and the experiment is achieved. Good agreement is also obtained when comparing the numerically and experimentally determined maximum forces of the hybrid components. The largest deviations are evident for the coating with an inner diameter of 24 mm and an outer diameter of 35 mm. Experimentally, a process force of 154.6 ± 0.6 kN is obtained, while the maximum force with 147.5 kN is underestimated in the simulation. However, with a deviation of 4.6 % from the experimentally determined results, a good agreement can be assumed here as well. The influence of the coating on the maximum process force is negligible. The deviations of the variations are within the standard deviation.

In addition to the maximum process forces, the geometry of the part, which was obtained experimentally and calculated numerically, is also compared. The basis for the comparison is the sheet thickness, which was determined at a drawing depth of 30 mm. The sheet thicknesses for the uncoated blank and for the coated blank with an inner diameter of 32 mm and an outer diameter of 43 mm of the coating are shown in Fig. 6. Since only a quarter model was built in the simulation, the resulting thicknesses are mirrored on the y-axis.

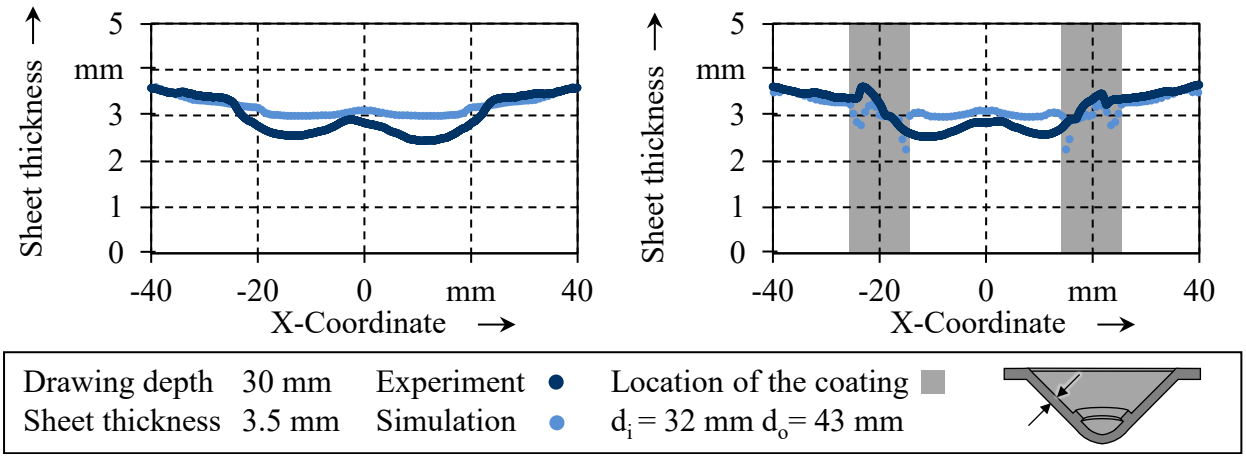

Fig. 6. Experimental and numerical sheet thickness distribution of the a) uncoated part and b) hybrid part.

A good agreement between simulation and experiment is found for the uncoated and the hybrid part in the area of the flange and in the radius area of the die. Deviations are evident in the bottom area of the conventional component. Here, the sheet thickness is overestimated in the simulation for both areas. The reason for this could be the modeling approach of the sheet with shell elements, which is only sufficiently accurate for a sheet with a thickness of 3.5 mm. This upper limit is reached in this case due to the use of a semi-finished part with a sheet thickness of 3.5 mm. Thus, the improvement of the accuracy of the model by using solid elements instead of shell elements has to be verified in future investigations. However, the areas in which the sheet thins out are correctly modeled. Moreover, the determination of the occurring stress states, which is the focus of this contribution, is mainly linked to the process forces, for which only small deviations of less than 5 % are identified. Therefore, it is assumed that the accuracy is adequate for the evaluation of the stress states and the use of the model for further investigations is possible.

Resulting stresses. Different stress states occur during deep drawing. Due to the use of a hemispherical punch, the stress conditions differ from those in conventional deep drawing.

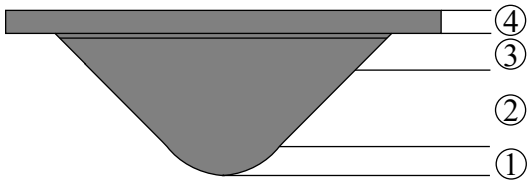

No.	Area	Stresses
1	Punch radius	Biaxial tensile
2	Transition zone	Plane strain/ uniaxial tension
3	Die radius	Bending
4	Flange area	Tensile compressive

Fig. 7. Resulting areas and stress states of a deep drawn part with a hemispherical punch.

The resulting stress states and the corresponding areas are shown in Fig. 7. The bottom area of the part is characterized by biaxial tensile stresses, similar to conventional deep drawing. The subsequent transition area is initially characterized by a plane strain area. As the punch diameter increases, uniaxial tensile stresses occur. In the area of the die radius, the material undergoes a double bending. In the flange area of the component tensile-compressive stresses occur.
By varying the diameter of the coating, it lies in different areas of the deep-drawn component and thus undergoes different stress states. In the following, the influence of the coating diameter on the resulting stresses is investigated. Since radial tensile and compressive stresses occur predominantly in the formed component, the direction-dependent stresses are considered. The resulting stresses in x-direction at a drawing depth of 30 mm and the interface pressure between the punch and the part are shown in Fig. 8.

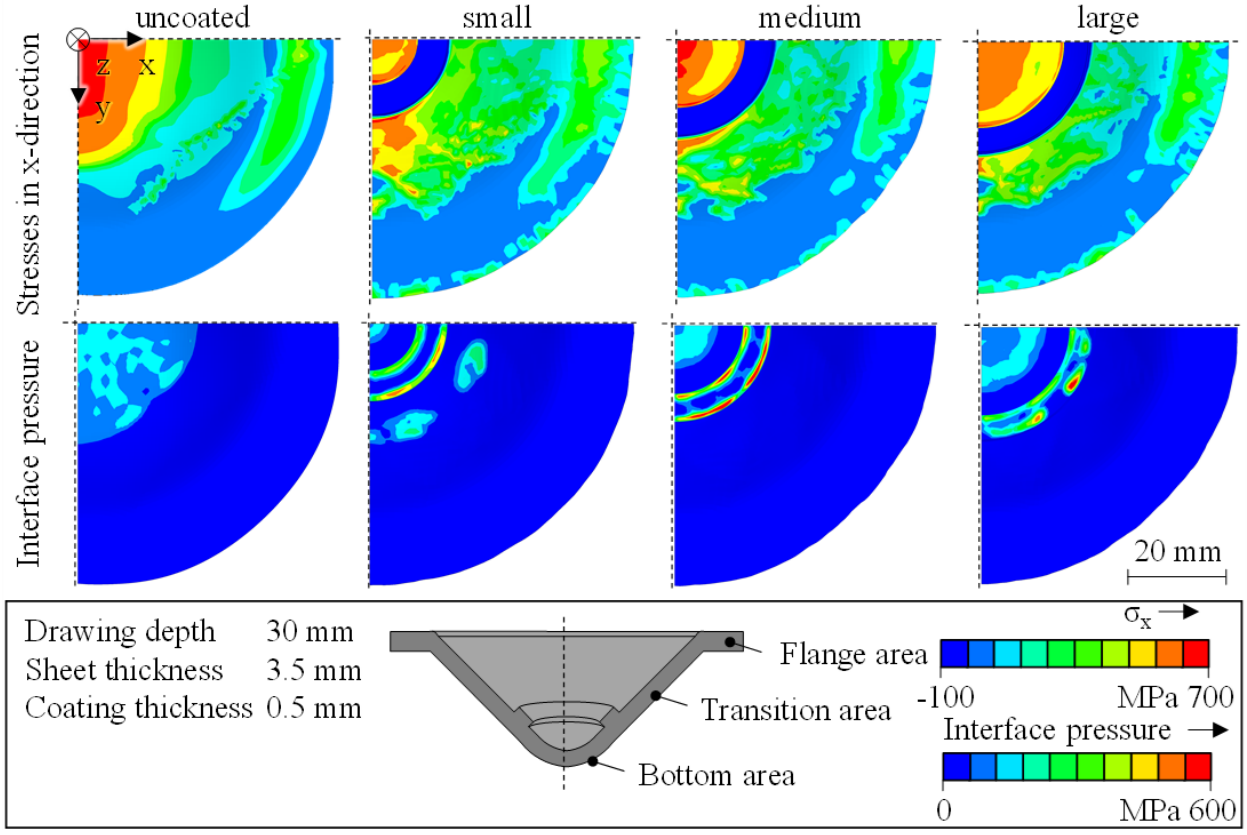

Fig. 8. Comparison of the resulting stresses in x-direction and the interface pressure between the part and the punch in the numerical deep drawing process of the conventional and hybrid parts with coating different diameters.

The maximum tensile stresses occur at the bottom area of the uncoated part. These are more dominant in the y-direction than in the x-direction. The bottom of the component is the most critical area in terms of the formation of cracks due to the maximum stresses in this area. Through the addition of the additively applied coating, the stresses in the bottom area are reduced. The reason for this is the loss of contact with the bottom of the component, as the punch primarily contacts the coating. With an increasing coating diameter, the punch has more contact with the bottom of the component. Therefore, the stresses in the bottom area of the hybrid part increase as well. The use of a coating, however, leads to stress peaks that occur at the inner and outer diameter of the coating, which can be critical regarding a failure of the part at higher drawing depths. A

bigger diameter of the coating leads to lower stresses around the coating. In addition to the stresses in x-directions, the major and minor strains of each finite element are investigated in order to evaluate the stress states of the component. The strains were determined numerically and are shown in Fig. 9.

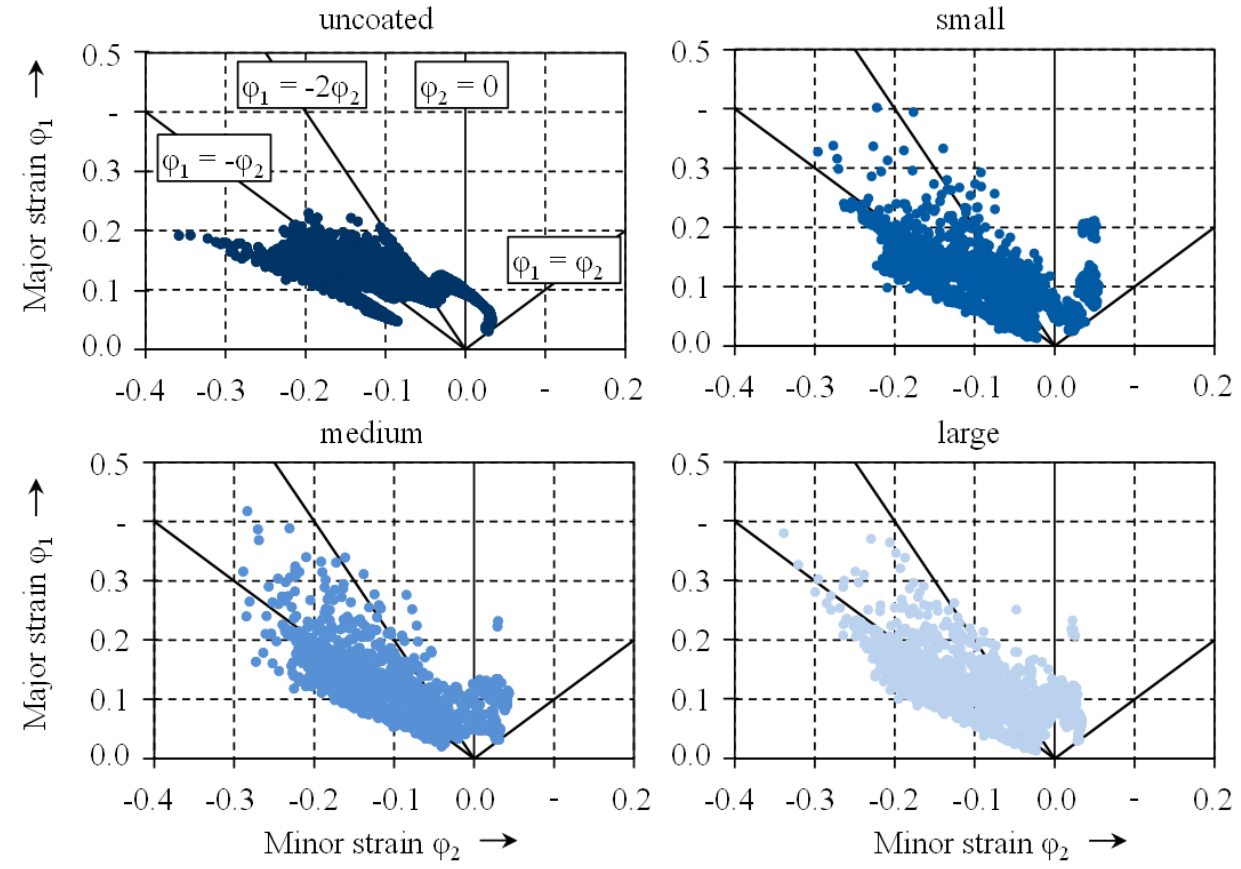

Fig. 9. Major and minor strains from the numerical investigations for the uncoated and hybrid parts.

In the uncoated component, positive major strains and negative minor strains are predominant. This is also observed for the hybrid parts. In the area of the coating positive major and minor strains occur. The major strains are higher at the inner and outer diameter of the coating, especially when using the small coating, and therefore more critical regarding failure. With a bigger diameter of the coating, the load on the coating is more in the area of plane strain with lower major strains. Placing the coating in the plane strain area is therefore more advantageous in terms of formability. Overall, the position of the coating can be used to influence the stress states in the bottom area of the hybrid part. The tensile stresses at the bottom area are reduced through the application of the additive coating. A bigger diameter of the coating leads to reduced stress peaks around the coating, which is due to the plane strain stress condition.

Summary

One approach to meet climate challenges is the combination of different production technologies in order to produce components more resource efficient. An example for this combination is the investigated process chain. In order to evaluate the influence of the additively applied coating on the forming process, a numerical model was built and validated by comparison with experimental

results. A comparison of the resulting maximum process forces from simulation and experiment showed good agreement. There were significant differences in the distribution of the sheet thickness, which can be explained by the modeling approach of the sheet using shell elements. Since the stress state depends mainly on the process force, the model was nevertheless qualified for these investigations. The use of the coating led to reduced tensile stresses in the bottom area of the hybrid component. An enlargement of the diameter of the coating helped to reduce the stress peaks around the coating. A bigger diameter of the coating also led to lower major strains in the area of plane strain. In further investigations, the modeling approach of the sheet with solid elements should be examined. It would also be of interest to model the heat affected area between the coating and the substrate in order to represent the real process more accurately and to better evaluate the influence of the coating.

Acknowledgement
The authors would like to thank the German Federal Ministry for Economic Affairs and Energy for funding the joint project HyConnect (FKZ: 03LB3010*), within the framework of which the present investigations were carried out. Furthermore, the authors would like to thank the Deutsche Edelstahlwerke Specialty Steel GmbH & Co. KG for providing the powder material and the Schaeffler AG for providing the substrate material for the tests.

References
[1] European Commission, A European Green Deal, 2022. https://ec.europa.eu/info/strategy/priorities-2019-2024/european-green-deal_en
[2] A.E. Tekkaya, N.B. Khalifa, G. Grzancic, R. Hölker, Forming of Lightweight Metal Components: Need for New Technologies, Procedia Eng. 81 (2014) 28-37. https://doi.org/10.1016/j.proeng.2014.09.125
[3] F. Klocke, Manufacturing Processes 4, Springer Berlin Heidelberg, Berlin, Heidelberg, 2013.
[4] I. Gibson, D. Rosen, B. Stucker, Additive Manufacturing Technologies, Springer New York, New York, NY, 2015.
[5] M. Merklein, D. Junker, A. Schaub, F. Neubauer, Hybrid Additive Manufacturing Technologies – An Analysis Regarding Potentials and Applications, Phys. Procedia 83 (2016) 549-559. https://doi.org/10.1016/j.phpro.2016.08.057
[6] M. Bambach, A. Sviridov, A. Weisheit, J. Schleifenbaum, Case Studies on Local Reinforcement of Sheet Metal Components by Laser Additive Manufacturing, Metals 7 (2017) 113. https://doi.org/10.3390/met7040113
[7] DIN EN ISO 6892-1:2020-06, Metallic materials - Tensile testing - Part 1: Method of test at room temperature, Beuth publishing, Berlin.
[8] C. Tome, G.R. Canova, U.F. Kocks, N. Christodoulou, J.J. Jonas, The relation between macroscopic and microscopic strain hardening in F.C.C. polycrystals, Acta Metall. 32 (1984) 1637-1653. https://doi.org/10.1016/0001-6160(84)90222-0
[9] J.E. Hockett, O.D. Sherby, Large strain deformation of polycrystalline metals at low homologous temperatures, J. Mech. Phys. Solid. 23 (1975) 87–98. https://doi.org/10.1016/0022-5096(75)90018-6
[10] M. Kreß, D. Bartels, M. Schmidt, M. Merklein, Material Characterization of Hybrid Components Manufactured by Laser-Based Directed Energy Deposition on Sheet Metal Substrates, KEM 926 (2022) 80–89. https://doi.org/10.4028/p-3vlx01
[11] J. Hafenecker, T. Papke, F. Huber, M. Schmidt, M. Merklein, Modelling of Hybrid Parts Made of Ti-6Al-4V Sheets and Additive Manufactured Structures, in: B.-A. Behrens, A. Brosius, W. Hintze, S. Ihlenfeldt, J.P. Wulfsberg (Eds.), Production at the leading edge of technology,

Springer Berlin Heidelberg, Berlin, Heidelberg, 2021, pp. 13-22. https://doi.org/10.1007/978-3-662-62138-7_2